Published online 7 January 2010

Nucleic Acids Research, 2010, Vol. 38, No. 7 ***2291–2301***
doi:10.1093/nar/gkp1210

Analysis of the impact of a uracil DNA glycosylase attenuated in AP-DNA binding in maintenance of the genomic integrity in *Escherichia coli*

Sanjay Kumar Bharti[1] and Umesh Varshney[1,2,*]

[1]Department of Microbiology and Cell Biology, Indian Institute of Science, Bangalore 560012 and [2]Jawaharlal Nehru Centre for Advanced Scientific Research, Bangalore 560064, India

Received August 9, 2009; Revised and Accepted December 15, 2009

ABSTRACT

Uracil DNA glycosylase (Ung) initiates the uracil excision repair pathway. We have earlier characterized the Y66W and Y66H mutants of Ung and shown that they are compromised by ~7- and ~170-fold, respectively in their uracil excision activities. In this study, fluorescence anisotropy measurements show that compared with the wild-type, the Y66W protein is moderately compromised and attenuated in binding to AP-DNA. Allelic exchange of *ung* in *Escherichia coli* with *ung*::*kan*, *ungY66H*:*amp* or *ungY66W*:*amp* alleles showed ~5-, ~3.0- and ~2.0-fold, respectively increase in mutation frequencies. Analysis of mutations in the rifampicin resistance determining region of *rpoB* revealed that the Y66W allele resulted in an increase in A to G (or T to C) mutations. However, the increase in A to G mutations was mitigated upon expression of wild-type Ung from a plasmid borne gene. Biochemical and computational analyses showed that the Y66W mutant maintains strict specificity for uracil excision from DNA. Interestingly, a strain deficient in AP-endonucleases also showed an increase in A to G mutations. We discuss these findings in the context of a proposal that the residency of DNA glycosylase(s) onto the AP-sites they generate shields them until recruitment of AP-endonucleases for further repair.

INTRODUCTION

Uracil DNA glycosylase (Ung), a ubiquitous enzyme, removes the promutagenic base uracil which appears in the genome either by deamination of cytosine or by incorporation of dUMP during DNA replication (1–3). Ung proteins belong to a highly conserved class of repair enzymes which are extremely specific for uracil in DNA (4,5). Ung proteins from *Escherichia coli* and other sources are inhibited by the reaction products, AP-DNA and uracil with K_i of ~1.2 μM and ~0.2–5 mM, respectively (3,6–10). Ung proteins are also inhibited by a *Bacillus subtilis* phage protein, Ugi (11). The complex formation of Ugi (which is a remarkable mimic of DNA) with *E. coli* Ung has been well characterized and shown to be extremely stable (12–14).

Ung initiates uracil excision repair by cleaving the *N*-glycosidic bond between the uracil base and the deoxyribose sugar in DNA. The AP sites so generated are further processed by AP endonucleases (15). A major pathway in *E. coli* employs the multifunctional enzyme, exonuclease III or the endonuclease IV to hydrolyse the phosphodiester bond 5′ to the abasic deoxyribose sugar to generate a 3′ hydroxyl, and a 5′ deoxyribose ends at the site of damage. A deoxyribose-phosphodiesterase (dRpase) activity (e.g. RecJ) is then utilized to cleave the deoxyribose to generate a 5′ phosphate end (16,17). The 5′ phosphate end can also result from β elimination of the deoxyribose, a reaction promoted by Fpg (18). The single nucleotide gap surrounded by 3′ hydroxyl and 5′ phosphate ends is then filled in by DNA polymerase I and sealed by DNA ligase to restore the locus sequence (16,17). AP lyases (e.g. endonuclease III) may also process the AP sites by cleaving 3′ to the AP site and generating a 5′ phosphate end. Although such a reaction bypasses the requirement of dRpase, it requires further processing of the 3′-end (e.g. by exonuclease III or endouclease IV) to convert it to a 3′ hydroxyl end to serve as primer for the DNA polymerase (19,20). In an alternate pathway, even though the 5′–3′ exonuclease activity of DNA polymerase I is unable to remove the 5′ deoxyribose, it can still carry out the fill in reaction (from the 3′ hydroxyl end) by replacement synthesis, and remove the 5′ flank containing the deoxyribose residue as a part of the DNA oligomer by

*To whom correspondence should be addressed. Tel: +91 80 2293 2686; Fax: +91 80 2360 2697; Email: uvarshney@gmail.com; varshney@mcbl.iisc.ernet.in

its structure specific endonuclease activity. The nicks so generated are sealed by DNA ligase (17). Other minor pathways involving nucleotide excision repair proteins have also been observed to repair AP sites in DNA (21,22). Importantly, AP sites are impediment to the essential cellular processes such as replication and transcription, and their accumulation in DNA is both mutagenic and cytotoxic (23–26). Therefore, a rapid processing of the AP sites is crucial to ensure that their occurrences in DNA are transient.

Analysis of human UNG binding to AP-site, and uracil containing DNAs showed that it bound to AP-DNA with an affinity higher than that with uracil containing DNA. It was also observed that the presence of AP endonuclease (HAP1) in the reaction, facilitated uracil excision repair. These observations led to the proposal that UNG-mediated uracil excision and the subsequent AP site processing are coupled (27). Accordingly, UNG would remain bound to the AP site until it was encountered by an AP endonuclease for its further processing. An inherent elegance of such a mechanism is that it ensures that AP sites are shielded, and prevented from eliciting mutator or cytotoxic effects (27,28). However, more recently, it was also reported that neither the human nor the Herpes simplex virus UNG bound AP-DNA better than the uracil containing DNA, implying implausibility of a coupled action of UNG and AP endonuclease (29). Although, it should be pointed out that to our knowledge, there are no reports which have addressed the issue of the *in vivo* implications of the altered Ung affinity/binding to AP-DNA in DNA repair.

We have been studying Ung-mediated repair in *E. coli*. In our earlier work, we reported on the mutational analysis of Y66 of the water activating loop (GQDPYH) in the active site pocket of Ung and showed that Y66W mutation compromised its activity by only about 7-fold (at the level of catalytic rates). Importantly, like the wild-type protein the Y66W mutant retained high specificity to uracil in DNA. However, unlike the wild-type protein, it was found to be recalcitrant to inhibition by uracil and AP-DNA (30). Another mutant, Y66H was severely compromised (~170-fold) in its uracil excision activity but like the wild-type protein, it was susceptible to inhibition by uracil and AP-DNA. In this study, we have exploited these mutants to address the issue of the significance of the Ung residency on the AP-site in the uracil excision repair pathway in *E. coli*.

MATERIALS AND METHODS

Oligodeoxyribonucleotides, bacterial strains, media and growth conditions

The DNA oligomers, plasmids and strains used are summarized in Table 1. 5′ FAM (referred to as fluorescein) labeled SSU9 (F-SSU9) DNA oligomer, was procured from Microsynth, Switzerland. Other DNA oligomers were from Sigma-Aldrich (India). The F-SSU9 oligomer was annealed to 3-fold molar excess of the 'complementary A' oligomer in 20 mM Tris–HCl (pH 7.5), 1 mM Na_2EDTA and 150 mM NaCl, heated at 80°C for 10 min and allowed to cool at room temperature to generate double-stranded oligomer (F-DSAU9) and stored at −20°C. *Escherichia coli* strains were grown in Luria–Bertani (LB) or LB-agar containing 1.6% (w/v) agar (Difco, USA). Media were supplemented with ampicillin (Amp, 100 μg ml^{-1}), kanamycin (Kan, 50 μg ml^{-1}) or rifampicin (Rif, 50 μg ml^{-1}) as required.

Expression and purification of Ung proteins

The pET11d derived expression constructs (30) were used to overproduce Ung from *E. coli* BL21 (DE3). Proteins were purified (31) and stored in 20 mM Tris–HCl, pH 7.5 and 10% glycerol. The pTUNG(Y147A) plasmid, a kind gift from Dr H. E. Krokan, Department of Cancer Research and Molecular Medicine, Norwegian University of Science and Technology, Norway, was used to purify a human (Hs) UNG (Y147A) mutant from *E. coli* BW310 (*ung*$^{-}$) strain (32).

Determination of affinity of Ung proteins to AP-DNA

The binding affinity of Ung proteins for the AP-DNA generated from F-SSU9 was monitored by fluorescence anisotropy measurement (29) using a fluorometer (Jasco FP-777 or Spex Fluoromax 3) after stabilizing polarizer. DNA oligomers (AP-DNA) were taken at a concentration of 1 μM in 100 μl buffer A (20 mM Tris–HCl, pH7.5, 50 mM NaCl, 0.1% BSA and 1 mM Na_2EDTA) along with Ung protein (5 μM to 200 μM) in a 0.2 ml quartz cuvette. The measurements were performed in a constant wavelength mode in autopolarizer settings after selecting polarizer and anisotropy with dark correction enabled. The excitation and emission wavelengths were fixed as 493 and 517 nm. The observed anisotropy was plotted against the concentration of enzyme, and the data were fitted to the quadratic binding equation, $A = A_{min} + [(D + E + K_D) - \{(D + E + K_D)\,2 - (4DE)\}\,1/2]\,(A_{max} - A_{min})/(2D)$, where (D) is the concentration of DNA used, (A) is the observed anisotropy, (A_{min}) is the anisotropy of free DNA and (A_{max}) is the anisotropy of protein bound DNA, (K_D) is the equilibrium dissociation constant and (E) is the total protein concentration.

Competitive binding of Ugi to Ung–DNA complex

To ascertain the specificity of Ung to AP-DNA, competitive binding of Ugi was performed by fluorescence anisotropy. Ung proteins (wild-type, 60 μM; Y66W, 50 μM; and Y66H, 88 μM) were taken along with the fixed concentrations of fluorescein-labeled AP-DNA (0.3 μM) corresponding to anisotropy values of 0.105, 0.14, 0.13, respectively and titrated against increasing concentration of Ugi. The scatter plot of titration with Ugi was generated by Sigma Plot 10, taking the maximum anisotropy of each protein as 100%.

Allelic exchange of *ung* in *E. coli* with the wild-type or the mutant genes

Genomic manipulations in *E. coli* were carried out using the method of Datsenko and Wanner (33), and P1

Table 1. List of strains, plasmids and DNA oligomers

Strain/Plasmids/Oligonucleotides	Details	Reference
E. coli Strains		
DY330	W3110 Δ*lacU169 gal490 λcl857*Δ(*cro-bioA*)	53
DY330 *ung*::*kan*	DY330 containing disruption of *ung* with *kan*^{R} cassette at BamHI site in the open reading frame (ORF).	This work
MG1655	An *E. coli* K strain, F$^-$ LAM$^-$ *rph*-1	54
MG1655 *ung*::*kan*	MG1655 containing *ung*::*kan* from DY330*ung*::*kan* strain	This work
MG1655 *ung*:*amp*	MG1655 wherein *ung* is linked with *amp*^{R} marker from the pTrc 99c vector.	This work
MG1655 *ungY66W*:*amp*	MG1655 wherein *ung* locus is replaced by *ungY66W*:*amp*	This work
MG1655 *ungY66H*:*amp*	MG1655 wherein *ung* locus is replaced by *ungY66H*:*amp*	This work
GM7635	AB1157 but Δ*xth-pncA nfo*-1::*kan ung*-152::Tn*10*.	35
GM7635 *ung*:*amp*	GM7635 wherein *ung*-152::Tn*10* locus has been replaced by *ung*:*amp*	This work
GM7635 *ungY66W*:*amp*	GM7635 wherein *ung*-152::Tn*10* locus has been replaced by *ungY66W*:*amp*	This work
BL21 (DE3)	Harbors T7 RNA polymerase gene under the control of LacR	Novagen
Plasmids		
pUC4K	Multicopy *E. coli* plasmid containing a *kan*^{R} cassette	55
pTrc-*ung*	Ugi was removed from pTrcUDG1-Ugi (56) by HindIII and EcoRI, blunt ended, ligated and characterized by restriction mapping.	This work
pTrc-*ungY66W*	pTrc*Eco*Ung but Y66 of Ung is mutated to W66	This work
pTrc-*ungY66H*	pTrc*Eco*Ung but Y66 of Ung is mutated to H66	This work
pTrc-*ung*:*kan*	*E. coli ung* disrupted by kanamycin resistance cassette from pUC4k	This work
pAC-*ung*	PstI–EcoRI fragement (1.5 kb) containing *E. coli ung* from pTZ*ung* was cloned into a plasmid with pAC origin of replication compatible with the colE1 origin of replication.	Purnapatre & Varshney (unpublished data)
Oligonucleotides		
F-SSU9	5′ FAM labeled d(ctcaagtgUaggcatgcaagagct); U at 9th position	This work
F-SS*ap*9	d(ctcaagtg***ap***aggcatgcaagagct; generated by excising U from F-SSU9 by uracil DNA glycosylase activity.	This work
Complementary A	5′ agctcttgcatgcctAcacttgag 3′.	Lab stock
F-DSAU9	Double stranded oligomer containing AU pair at position 9, formed by annealing F-SSU9 with complementary A oligomer.	This study
F-DS*ap*9	Double stranded AP-DNA formed by excising U from F-DSAU9.	This study
ung-Fp	5′ d(atggctaacgaattaacc) 3′; anneals to *ung* form the start codon	Lab stock
*ung*UP-Fp	5′d(tggatacctgtaatcatg) 3′	38
pTrc-Bcl-Rp	5′ d(ggctgttttggcggatgagaga) 3′	
pTrc-*ung*-ko-Rp	5′ d(**ggtggcaactctgccatccggcatttccccgcaaatg**tggaacgaaaactcac) 3′. Sequences in bold correspond to the region downstream of *ung* ORF and the underlined sequence anneals to the sequence downstream of Amp^R cassette from pTrc99C.	This work
306 *rpoB*-Fp	5′d(cgaccacttcggcaaccg) 3′; Forward primer to amplify RRDR locus.	46
306 *rpoB*-Rp	5′ d(cgatcagaccgatgttgg) 3′; Reverse primer to amplify RRDR locus	46
Eco-*rpoB*-seq-Fp	5′ d(ggcgaaatggcggaaaac) 3′; Primer used to sequence RRDR	46
Eco-*ssb*-fp	5′ d(ggaattcaccatggccagcagagg) 3′; Forward primer used to amplify *E. coli* single-stranded DNA gene ORF.	40
Eco-*ssb*-rp	5′ d(gactgatcagaacggaatgtc) 3′; Reverse primer used to amplify *E. coli* single-stranded DNA gene ORF.	40

phage-mediated transductions (34). A DNA fragment harboring kanamycin resistance cassette (Kan^R; *kan*) was excised from pUC4K as BamHI fragment and subcloned into the BamHI site of the *ung* gene open reading frame (ORF) in pTrc-*ung* to generate pTrc-*ung*::*kan*. A DNA fragment harboring *ung*::*kan* was amplified from pTrc-*ung*::*kan* with *ung*-Fp and pTrc-Bcl-Rp primers using *Pfu* DNA polymerase. PCR reactions (50 µl) contained 1× Pfu buffer, 50–100 ng of template DNA, 20 pmol of each primer, and 200 µM of dNTPs. Reactions were heated at 94°C for 4 min and subjected to 29 cycles of incubations at 94°C for 1 min, 50°C for 30 s and 70°C for 10 min. PCR product of ∼1.88 kb was digested with BclI and electroporated into *E. coli* DY330. The transformants were selected on LB-agar containing Kan and the chromosomal *ung* gene disruption was confirmed by a diagnostic PCR. The strain, *E. coli* DY330 *ung*::*kan* so obtained was used for further manipulations.

To perform allelic exchange of the *ung*::*kan* locus in *E. coli* DY330 with the wild-type, Y66W and Y66H *ung* alleles, the *ung* ORF along with the downstream Amp^R marker from the respective pTrc99C-based constructs (Table 1) were amplified by PCR using *ung*-Fp and pTrc-*ung*-ko-Rp primers (Supplementary Figure S1) with *Pfu* DNA polymerase, under the conditions described above. The *ung*-Fp is completely homologous to the *ung* ORF upstream of the BamHI site, and the pTrc-*ung*-ko-Rp possesses sequence homologous to the vector sequence (downstream of the Amp^R marker) which is flanked on its 5′ side with a sequence homologous to the 3′ untranslated region of the *ung* gene. Use of these primers allows co-amplication of Amp^R marker located downstream of the desired *ung* alleles in the pTrc99C constructs. The PCR product was electroporated into the *E. coli* DY330 *ung*::*kan* strain and the transformants obtained by recombinational replacement of *ung*::*kan*

locus were selected by their Amp^R and Kan^S phenotype. The required *ung* loci from the *E. coli* DY330 were mobilized to *E. coli* MG1655 (wild-type strain) or GM7635 (an *exo*$^-$ *ung*$^-$ strain which was a kind gift from Dr Bevin P. Engelward, MIT, Cambridge, USA) (35) by P1 phage-mediated transductions with the help of the linked Amp^R marker. Chromosomal manipulations were confirmed by sequencing of the PCR product obtained using *ung*UP-Fp and pTrcBcl-Rp (Supplementary Figure S2).

Immunoblot analysis

Cell-free extracts were prepared as described (36). The extracts corresponding to 50 µg of total proteins were fractionated on SDS–PAGE (15%) and the middle region of the gel was electroblotted onto PVDF membrane (GE Healthcare). The membrane was blocked overnight with 5% non-fat dairy milk in TBST (20mM Tris–HCl, pH7.4, 0.2 % Tween 20, 150 mM NaCl), washed thrice with TBS and incubated with rabbit antiserum (1:2000 dilution) containing anti *Eco*Ung polyclonal antibodies for 2 h at room temperature. The membrane was washed thrice with TBS and incubated with anti-rabbit goat IgG secondary antibody conjugated with alkaline phosphatase at a dilution of 1:1000 for 2 h, washed again with TBS and developed with BCIP and NBT as substrate.

Determination of mutation frequencies

Isolated colonies were grown to early log phase (OD_{600}, 0.2–0.3) in 5 ml LB and diluted 1000 fold to make 6–7 independent cultures (5 ml). The cultures were grown to OD_{600} of ~0.6–1.0, and cells were harvested, resuspended in 100 µl LB, plated on LB agar containing Rif, incubated at 37°C overnight in dark and scored for the numbers of colonies that appeared (37). Total number of viable cells in each culture was determined using a linear regression equation, $Y = mx + C$, from a standard curve prepared in the beginning of the experiment by plotting OD_{600} and the total viable counts for the various strains.

Analysis of rifampicin resistance determining region

Escherichia coli strains in various backgrounds were grown for 10–12 h and plated on LB agar containing Rif. The isolated colonies were suspended in 20 µl water, incubated at 90°C for 10 min, spun at 13 000 r.p.m. for 10 min in table top centrifuge and the supernatant was used as a template to amplify rifampicin resistance determining region (RRDR) using 306 *rpoB*-Fp and 306 *rpoB*-Rp primers (Table 1). PCR reactions (40 µl) contained, 1× Taq pol buffer, 10 µl of template, 15 pmol of each primer, 150 µM of dNTPs and 0.75 U of Taq DNA polymerase. The PCR condition were as follows, initial denaturation at 94°C for 4 min, followed by 29 cycles of denaturation at 94°C for 1 min, annealing at 55°C for 30 s, polymerization at 68°C for 30 s and final extension at 68°C for 10 min. The PCR products were electrophoresed on 1% agarose gel and eluted in 0.2% low-melting agarose. DNA sequencing was done by Macrogen Inc. (Seoul, Korea) using Eco-*rpoB*-seq-Fp.

Modeling of thymine in the active site pocket of Ung

Thymine was modeled into the mutant Ung proteins by the method of Coot (38). The models of Y66W Ung and Y147A HsUNG were generated from the crystal structure with the PDB coordinate files 1FLZ and 1SSP, respectively and the rotamer selection for Trp was performed as reported earlier (30). The models obtained for the Y66W Ung and thymine accommodated Y66W were energy minimized in vacuum with low memory Broyden–Fletcher–Goldfarb–Shanno approach to remove any unacceptable steric clash followed by conjugated gradient and steepest descent methods in the solvent system using GROMACS v3.3.1 (39). The models of thymine with Y66W and Y147A mutant proteins were generated after adding methyl group to the C5 of uracil.

Assay for thymine DNA glycosylase activity

The DNA substrate containing [^{3}H] radiolabeled thymine was prepared by PCR amplification of *ssb* gene using ORF specific Eco-*ssb*-fp and Eco-*ssb*-rp primers (40) to amplify 565 bp DNA using Taq DNA polymerase (~2 U), 50 ng of the template DNA, 20 pmol each of the forward and reverse primers, 20 µM [^{3}H] dTTP (GE healthcare, UK) and 200 µM dCTP, dATP and dGTP in a 50 µl volume. Reaction was heated to 94°C for 4 min and subjected to 29 cycles of incubations at 94°C for 1 min, 52°C for 30 s and 68°C for 40 s. Subsequently, the reaction was supplemented with 20 µl reaction buffer containing 10 pmol each of the primers, 100 µM all dNTP mix, Taq DNA polymerase (~2 U) and subjected to another round of 29 cycles of incubations as above. The reaction was loaded onto an agarose gel and the PCR product was purified by GFX PCR DNA and the gel band purification kit (GE Healthcare, UK). Thymine DNA glycosylase (TDG) activity was determined (41) by incubating 250 ng of the Ung proteins (pre-incubated with 150 ng of Ugi or buffer alone for 15 min at room temperature followed by 30 min on ice) with 25 000 c.p.m. of ^{3}H-labeled DNA substrate and incubated at 37°C for different times. At the end of the reaction, the samples were mixed with unlabelled thymine and spotted on the CEL 300 PEI/UV_{254} (POLYGRAM, Macherey-Nagel, Germany) thin layer plates, and developed with 2% formic acid (v/v) containing 0.55 M LiCl as the mobile phase at 4°C (42). The spots corresponding to thymine were visualized by UV (254 nm) shadowing and cut into pieces to measure the radioactivity by liquid scintillation counting using a fluid containing 0.5 g PPO (2,5-diphenyloxazole) and 0.05g POPOP [1,4-bis (5-phenyl-2-oxazolyl) benzene] per liter in toluene. The percentage of thymine released was calculated for each sample and plotted as histogram.

Genomic degradation assays

For the TDG activity-based DNA degradation assay, ~1.5 µg of genomic DNA from *E. coli* MG1655 (wild-type for *ung*) was mixed with 500 ng of the various Ung proteins (or their complexes with Ugi) and incubated at 37°C for 3 h. For uracil DNA glycosylase-based DNA

degradation assay, ~1.5 μg of genomic DNA from *E. coli* RZ1032 (*dut*$^-$ *ung*$^-$) was mixed with 200 ng of the proteins (or their complexes with Ugi) and incubated at 37°C for 15 min. The reactions were stopped with NaOH (0.1 N), heated for 10 min at 90°C, analyzed by electrophoresis on 1% agarose gel containing ethidium bromide (43) and documented using a gel doc system (Alpha Innotech Corporation).

RESULT

Binding of Ung proteins to AP-DNA

We have earlier observed that compared to the *E. coli* Ung (wild-type), its Y66W and Y66H mutants were about 7- and 170-fold, respectively compromised in their uracil excision activities. And, although the wild-type and the Y66H mutant were inhibited by the presence of AP-DNA, the Y66W was not (30). The latter observation indicated that Y66W was compromised and/or altered in its binding to AP-DNA. To verify this, we analyzed binding of these proteins to AP-DNA employing fluorescence anisotropy technique (29, 44). For this purpose, F-SS*ap*9 and F-DS*ap*9 containing an AP-sites at position 9 from the 5′-end-labeled with fluorescein were prepared by incubating the respective oligomers with the Ung proteins (wild-type, Y66W or the Y66H mutants) for 5 min at room temperature prior to recording equilibrium binding measurements. Expectedly, as shown in Figure 1A and B, such a treatment of F-SSU9 with the Ung proteins alone did not result in any significant cleavage of the oligomer [compare lane 1 (untreated) with lanes 2, 5 and 8, (treated with wild-type, Y66H and Y66W proteins, respectively)]. However, a further treatment with alkali or alkali and heat resulted in total shift of the upper bands in lanes 2, 5 and 8 into smaller 5′ fluorescein products (lanes 3, 4; 6, 7; and 9 and 10) suggesting that conditions used resulted in total excision of uracil from oligomers and generation of AP-DNA. In our initial experiments, we observed that binding of Ung proteins to F-SS*ap*9 resulted in increasing anisotropy values with respect to increasing protein concentration (data not shown). To ensure that the increase in anisotropy was due to a specific binding of the oligomer and not due to protein interference with the 5′ fluorescein label, we added Ugi, a *Bacillus subtilis* phage, PBS1 encoded highly specific proteinaceous inhibitor of Ung (which interacts in the DNA binding groove), to the reactions and monitored percent decrease in anisotropy with respect to the increasing concentration of Ugi (Figure 1C). Addition of Ugi competed with the complex of F-SS*ap*9 with the Ung proteins, suggesting that the anisotropy changes represent specific binding of the fluorescein-labeled oligomer.

Subsequently, the binding of Ung proteins to F-DS*ap*9, a substrate more akin to *in vivo* conditions, was observed by the increasing anisotropy values with respect to the increasing protein concentrations (Figure 1D and Supplementary Figure S3). The equilibrium binding of the wild-type and the mutant proteins were determined by fitting the data to a quadratic binding equation using Sigma plot. As shown, the K_D of Y66W mutant was ~4.5-fold higher when compared to the wild-type protein suggesting a somewhat weaker affinity of the Y66W Ung to AP-DNA. Under the same conditions, the Y66H Ung showed a K_D which was ~3-fold higher than that of the wild-type protein. In addition, we observed that, while the maximal anisotropy values of the wild-type and Y66H proteins were the same; that of the Y66W was significantly higher. Such differences in anisotropy values were also observed for the interaction of DNA oligomers with EcoRV and interpreted to imply an altered mode of DNA protein interaction (44). Taken together with our earlier observation that unlike the wild-type and the Y66H Ung, the Y66W Ung is not inhibited by either uracil or uracil and AP-DNA (30), these observations suggest that the mode of AP-DNA binding to the Y66W mutant is altered (attenuated).

Generation of *E. coli* strains harboring the desired *ung* alleles in chromosome

To ensure physiological relevance of the role of Ung binding in DNA repair, we replaced the chromosomally located *ung* gene in *E. coli* DY330 with the recombinant constructs using a two step allelic exchange method (see 'Materials and Methods' section). The *ung* alleles from *E. coli* DY330 were then moved into *E. coli* MG1655 background using genetic transductions and verified by DNA sequence analysis. Figure 2A shows the *ung* gene organization in the engineered strains. Although the *ung* alleles were introduced in their native location (58.51′) with minimal alteration, to ensure that the chromosomal manipulations did not result in any dysregulation of Ung expression, we carried out immunoblot analysis of the cell-free extracts prepared from the engineered and the parent strains using polyclonal antibodies against *E. coli* Ung. As shown in Figure 2B, expression of Ung proteins from the MG1655 parent strain and its derivatives harboring an Amp^R marker linked to the wild-type (*ung*:*amp*), Y66H (*ungY66H*:*amp*) and Y66W (*ungY66W*:*amp*) expressed equal levels of Ung proteins (compare lane 1 with lanes 2–4). And, as expected, the strain wherein the *ung* gene was disrupted with Kan^R marker (*E. coli* MG1655 *ung*::*kan*) did not show any bands corresponding to Ung (lane 5). As a control, the immunoblot was also simultaneously probed for RRF protein using polyclonal antibodies to RRF which confirmed equal loading of the samples, lanes 1–5).

Determination of mutation frequencies

To understand the impact of the mutations in the *ung* genes in *E. coli*, we determined mutation frequencies of the strains carrying the wild-type, Y66W, Y66H and the disrupted *ung* alleles by scoring for colonies (Rif^R) that appear on Rif containing LB-agar. As shown in Table 2, when compared with the wild-type strain (*ung*:*amp*), the *ung*− (*ung*::*kan*) strain showed an increase of 5.1-fold. This increase in the mutation frequency is similar to

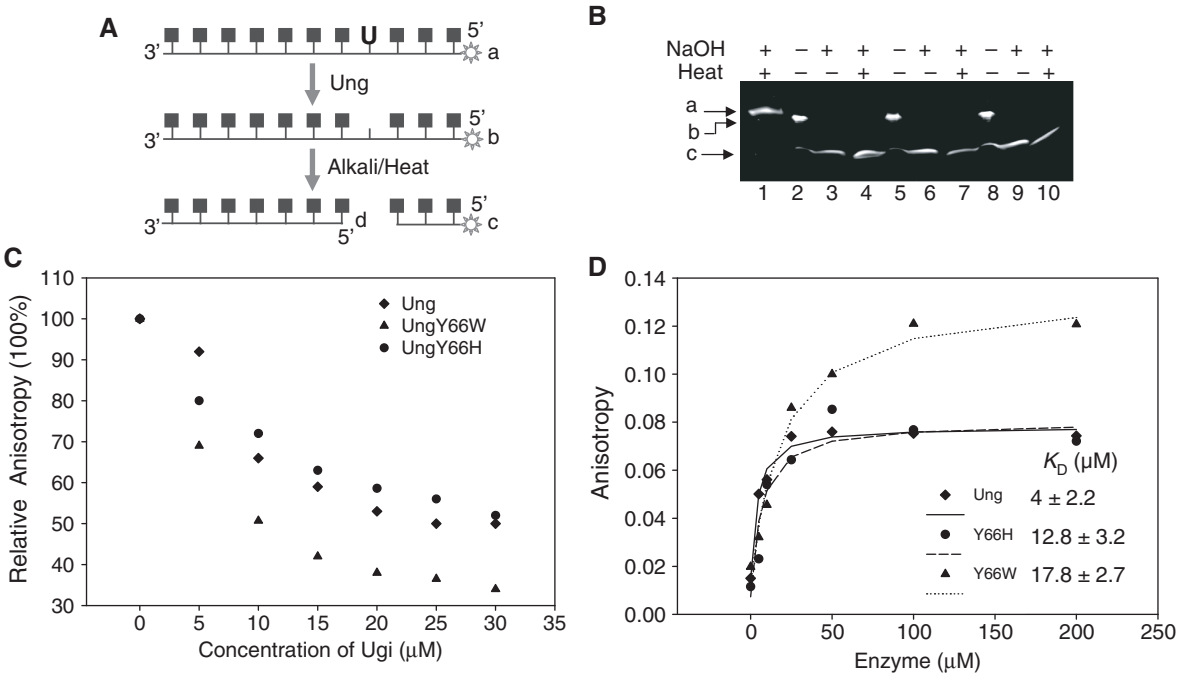

Figure 1. Generation of fluorescein-labled SS*ap*9 oligomer and its binding to the Ung proteins. **(A)** Scheme of uracil excision from F-SSU9 (a) to generate F-SS*ap*9 (b). Cleavage of F-SS*ap*9 (b) in the presence of alkali, or alkali and heat results in the formation of (c) and (d). Of these, (a), (b) and (c) are detectable on the gel shown in (B). **(B)** Analysis of uracil excision from F-SSU9 with Ung proteins. The DNA oligomer was incubated with Ung proteins (5 μM); aliquots were taken out and analyzed on 15% polyacrylamide–8 M urea gels before and after treatment with alkali and alkali and heat. Lane 1, untreated F-SSU9; Lanes 2, 5 and 8, F-SSU9 treated with wild-type, Y66W and Y66H Ung; lanes 3, 6 and 9, same as in lanes 2, 5 and 8, respectively after treatment with alkali; lanes 4, 7 and 10, same as in lanes 3, 6, and 9 after treatment with alkali and heat. **(C)** Determination of the specificity of F-SS*ap*9 binding to the Ung. Complexes of Ung proteins with F-SS*ap*9 (see 'Materials and Methods' section) were competed with increasing amounts of Ugi. Anisotropies, relative to the starting values of the respective complexes of F-SS*ap*9 with Ung proteins (taken as 100%, in the absence of Ugi) were plotted against Ugi concentration. **(D)** Fluorescence anisotropy measurements using a double-stranded AP-DNA. The F-DSAU9 (1 μM) was mixed with 5 μM to 200 μM Ung proteins (wild-type, filled diamond; Y66W, filled triangle; and Y66H, filled circle) and the flluorescence anisotropy was measured in Jasco FP-777. Data points were fitted to binding equation (see 'Materials and Methods' section). The K_D values shown are the averages from two experiments ± SEM.

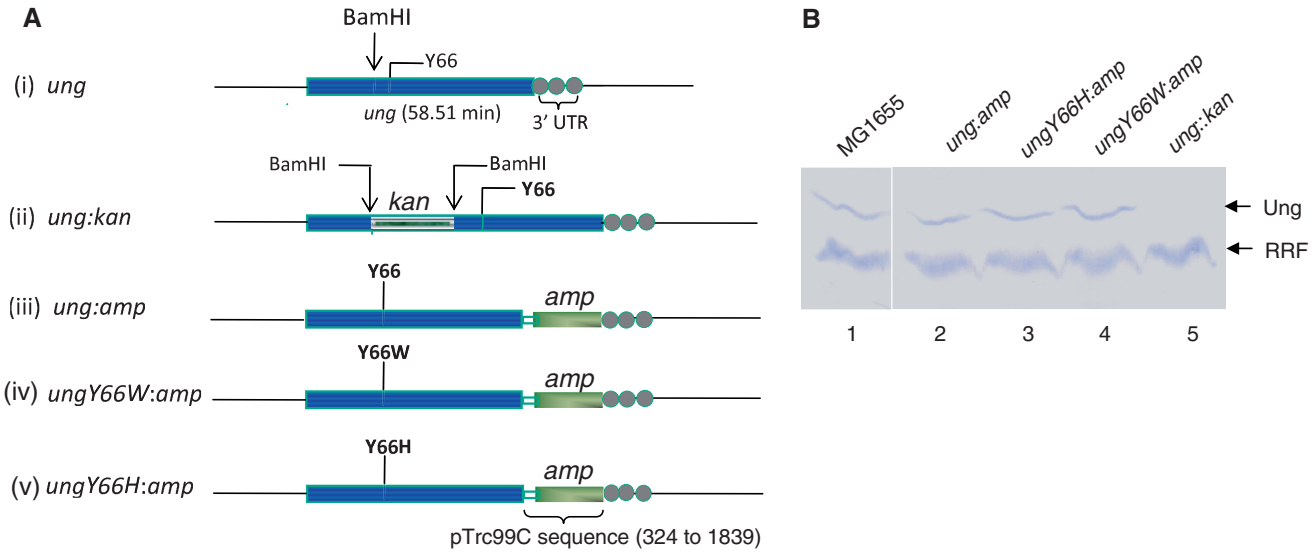

Figure 2. Characterization of *E. coli* MG1655 strains. **(A)** Genomic organization of *E. coli* MG1655 strains harboring various *ung* alleles. **(B)** Immunoblot analysis of the cell-free extracts using anti-Ung and anti-RRF antibodies. Cell-free extracts prepared from *E. coli* MG1655 strain (lane 1), or its derivatives harboring amp^R linked wild-type (*ung*:*amp*, lane 2), Y66H (*ungY66H*:*amp*, lane 3), Y66W (*ungY66H*:*amp*, lane 4) and *ung*- (*ung*::*kan*, lane 5) alleles.

those reported earlier for *ung*− strains of *E. coli* (45). Under the same conditions, the Y66H (*ungY66H*:*amp*) strain which encodes an Ung ~170-fold compromised in its activity showed an increase of ~2.8-fold in mutation frequency, suggesting that even a highly compromised Ung could partially rescue the phenotype of a null strain. Interestingly, the mutation frequency of the strain harboring the Y66W allele, which is merely ~7-fold compromised in its activity also showed a nearly similar increase of ~1.8-fold.

Determination of mutations in RRDR of *rpoB*

To gain further insights into the mechanistic aspects, we determined the mutation spectrum in the RRDR locus of the *rpoB* gene in the Rif^R colonies obtained from the strains harboring either a wild-type, Y66W or Y66H alleles of *ung*. Data are shown in Supplementary Figure S4, and summarized in Table 3. As reported (41,46), predominant mutations in the wild-type *ung* background (MG1655, *ung*:*amp*) belonged to C to T transitions (58%). Expectedly, the strain with Y66H allele which is about 170-fold compromised in its Ung activity (MG1655, *ungY66H*:*amp*), showed an almost exclusive occurrence of C to T mutations (96%). However, the mutations in the Y66W background (MG1655, *ungY66W*:*amp*) corresponded predominantly to A to G category (63.5%) which is quite distinct from that of the strains harboring either the wild-type or the Y66H alleles. Further, we noticed that A to G changes were also a predominant cause of Rif^R mutations in a strain, deficient for exonuclease III and endonuclease IV (Table 3; GM7635, *ung*:*amp*; and *ungY66W*:*amp*).

Table 2. Mutation frequencies of *E. coli* MG1655 strains harboring wild-type (*ung:amp*), Y66H (*ungY66H*:*amp*), Y66W (*ungY66H*:*amp*) and *ung*- (*ung*::*kan*) alleles of *ung*

Strain	Mutation Frequency ($\times 10^{-7}$)	Fold increase
ung:*amp*	4.9 ± 1.6	1
ung::*kan*	25 ± 2.4	5.1
ungY66W:*amp*	8.9 ± 1.7	1.8
ungY66H:*amp*	19.7 ± 1.9	2.8

Y66W lacks TDG activity

Expression of human (Hs) UNG (Y147A) mutant, wherein mutation of Y147 (equivalent of Y66 of *E. coli* Ung) to Ala resulted in acquisition of a weak TDG activity, showed a prominent increase in A to G mutations in the RRDR locus in *E. coli* (41). Our earlier studies suggested that the Y66W mutation in *E. coli* Ung resulted in widening of the uracil binding pocket (30). Although, in an oligonucleotide-based assay thymine excision activity of the Y66W mutant was not detected, it was important to rule out a possibility of minor TDG activity. Hence, we employed the ^{3}H-thymine release assays used earlier to detect the weak TDG activity of the Y147A mutant of HsUNG (41). As shown in Figure 3, the wild-type Ung (columns 1 to 4) showed the presence of ~2.5% free ^{3}H thymine in the reactions irrespective of the absence or presence of Ugi or the time of incubation (1 h or 5 h), suggesting that this was the background level of free thymine in our assays. The Y66W Ung (columns 5 to 8) mutant also showed very similar levels of free ^{3}H thymine in such reactions. Expectedly, as observed before (41), in the assays with the Y147A mutant of HsUNG, we could detect increasing

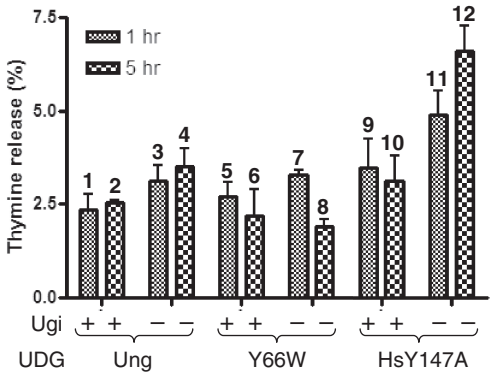

Figure 3. *In vitro* excision of [^{3}H] thymine from DNA. [^{3}H] thymine containing DNA was incubated with the various Ung proteins (or their complexes with Ugi) for the indicated times. The thymine release was analyzed by chromatography on PEI thin layer plates, calculated as percentage release [(free thymine)/(free thymine + DNA substrate left)]*100 from three different experiments, and plotted as histograms. Error bars indicate standard deviation.

Table 3. Spectrum of mutations in RRDR locus of rifampicin resistant isolates of different strains of *E. coli*

Strain background	RRDR loci sequenced mutant (total)	C to T % (no.)	A to G % (no.)	A to T % (no.)	C to A % (no.)	A to C % (no.)	C to G % (no.)
MG1655							
ung:amp	48 (58)	58 (28)	17 (8)	17 (8)	8 (4)	0	0
ungY66W:*amp*	41 (57)	22 (9)	63.5 (26)	2.5 (1)	9.5 (4)	0	2.5 (1)
ungY66H:*amp*	46 (55)	96 (44)	4% (2)	0	0	0	0
MG1655 + pAC*ung*							
ung:amp	48 (48)	40 (19)	14.5 (7)	14.5 (7)	27 (13)	2 (1)	2 (1)
ungY66W:*amp*	52 (56)	42 (22)	21 (11)	10 (5)	10 (5)	15 (8)	2 (1)
GM7635							
ung:amp	40 (58)	12.5 (5)	65 (26)	12.5 (5)	7.5 (3)	0	2.5 (1)
ungY66W:*amp*	40 (50)	20 (8)	40 (16)	2.5 (1)	35 (14)	2.5 (1)	0

amounts of thymine release in the reactions (columns 11 and 12). Interestingly, such an increase in thymine release was not seen (columns 9 and 10) when the Y147A mutant was pre-incubated with Ugi, a phage protein which sequesters the protein into an inactive complex, suggesting that although the level of thymine release was small, it was due to the specific TDG activity of the Y147A mutant reported earlier (41).

Moreover, we reasoned that the Y147A mutant, due to its TDG activity should cleave the glycosidic bond between a thymine and the sugar from the genomic DNA (from wild-type *E. coli*) leading to generation of AP sites (which are susceptible to alkaline pH) in the DNA. As shown in Figure 4A, treatment of the genomic DNA with NaOH and heat alone results in denaturation of the DNA which migrates as a smear in high molecular weight region of the gel (compare lane 2 with 1). However, compared with this buffer control (lane 2), assays with the Y147A HsUNG (lane 8) but not the wild-type or the Y66W proteins (lanes 4 and 6) resulted in degradation of the DNA to a faster migrating species. Also, the DNA degradation activity of the Y147A mutant was inhibited by its pre-incubation with Ugi (lane 7). As a control, we performed a similar assay using uracil containing genomic DNA isolated from *E. coli dut*$^{-}$*ung*$^{-}$ strain (Figure 4B). As expected, assays with all the three proteins resulted in degradation of the DNA (compare lanes 4, 6 and 8 with 2). And, when the proteins were pre-incubated with Ugi, the DNA degradation activity of all the proteins was inhibited (lanes 3, 5 and 7).

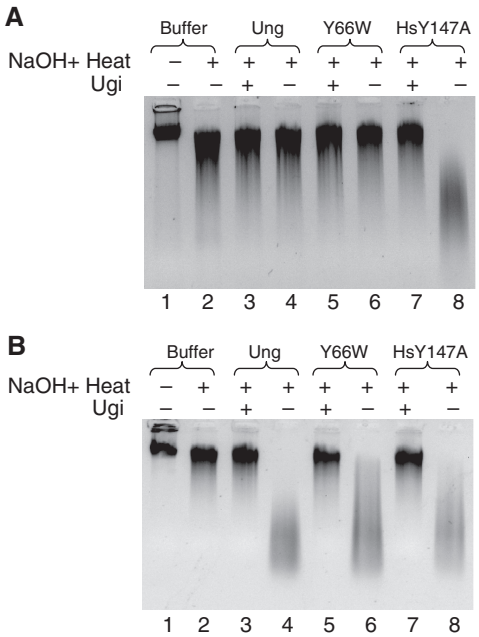

Figure 4. Genomic degradation assays. (**A**) The genomic DNA (~1.5 μg) from *E. coli* (wild-type for *ung*) was mixed with buffer alone (Buffer) or 500 ng of wild-type *Eco*Ung (Ung), Y66W *Eco*Ung (Y66W), Y147A mutant of human UNG (HsY147) in the absence (−) or the presence (+) of Ugi, incubated at 37°C for 3 h, treated with NaOH and heat, and analyzed by electrophoresis on agaraose gel and recorded. (**B**) Same as (A) except that the genomic DNA was from *dut*$^{-}$*ung*$^{-}$ strain of *E. coli* and the amount of Ung proteins used was 200 ng, and the reactions were done for 15 min.

Finally, we used the crystal structure of the complex of *E. coli* Ung with uracil to generate a model of Y66W. The substitution of tyrosine with tryptophan (a bigger side chain) was followed by energy minimization to generate a sterically acceptable model. As reported earlier (30), the uracil binding pocket of the Y66W mutant was widened due to movement of 72–82 polypeptide segment away from the centre of binding pocket. However, docking of thymine into the model resulted in a severe unacceptable steric clash with the tryptophan side chain (Supplementary Figure S5A). In fact, it was not possible to accommodate thymine in any other configuration without unacceptable changes in the conformations of the active site residues in the binding pocket (Supplementary Figure S5C). Interestingly, as expected from the experimental data (Figures 3 and 4; and ref. 41), a similarly generated model of HsY147A UNG, having a smaller side chain at this position, using the co-ordinates of the co-crystal structure of HsUNG with U-containing DNA substrate, showed that it accommodated thymine without any steric clash (Supplementary Figure S5B).

Taken together, the data in Figures 3, 4 and Supplementary Figure S5 suggest that the Y66W Ung (like its wild-type counterpart) shows strict specificity for uracil in DNA, and that it has not acquired any unspecific base excision activities.

Overexpression of the wild-type Ung in the *ungY66W*:*amp* strain mitigates occurrence of A to G mutations

To obtain an *in vivo* evidence to support that the increase in A to G mutations in the *ungY66W*:*amp* is a consequence of the uracil excision activity of the Y66W protein, we overexpressed the wild-type Ung in the *ungY66W*:*amp* strain from a medium copy plasmid (pAC-*ung*). As the wild-type Ung is strictly specific for uracil excision, we reasoned that such an expression of the wild-type protein would compete with the Y66W protein for its uracil excision activity (but no other base excision activity, if any).

Interestingly, while the expression of wild-type Ung did not result in any significant alteration in the mutation spectrum in the wild-type strain background (Table 3; MG1655 + pAC-*ung*, *ung*:*amp*), it mitigated the occurrence of A to G mutations (from 63.5% to 21%) in the *ungY66W*:*amp* strain (MG1655 + pAC-*ung*, *ungY66W*:*amp*) suggesting that the A to G mutations in this (*ungY66W*:*amp*) background were indeed a consequence of uracil excision by the Y66W mutant. In fact, had the unspecific base excision activity (undetectable by the *in vitro* assays) of the Y66W been responsible for the A to G mutations, the occurrence of these mutations could have even increased upon overexpression of the wild-type Ung.

DISCUSSION

The genomic integrity in cells is constantly endangered by the damages inflicted upon DNA at various levels during normal cellular physiology. Damages such as the base

modifications (e.g. deamination, methylation and oxidation) or their total elimination from DNA are of common occurrence. For a mammalian cell genome, spontaneous occurrence of events leading to generation of AP sites have been estimated to be as high as 100 000 per day (2). Based solely on this estimate, a genome of the size present in *E. coli* would incur about a dozen AP sites per day. However, because of the high metabolic rates, their actual numbers may far exceed this estimate. The reactive nitrogen and oxygen species generated as a part of normal physiological activity of the cell are the major agents that damage DNA (47–49). In addition, a number of DNA glycosylases produce AP-DNA as an intermediate during the repair process. As the AP sites are a major threat to DNA integrity, and a cause of high rates of mutations and cytotoxicity, organisms invests quite prominently to production of enzymes that repair AP sites in the genome (23–26,41).

Binding of DNA glycosylases such as MutY (50,51), TDG (28), MUG (52), UdgB (46), human UNG (27), etc. to abasic sites has been demonstrated to be stronger than to their DNA substrates. Such a property of DNA glycosylases has been envisaged to play a role in the coupling between the DNA glycosylases and the downstream enzymes. According to the hypothesis, a DNA glycosylase could remain bound to the AP-site it generates until an AP endonuclease becomes available to process the site, and thus shield it from eliciting mutator effects. Such a coupling would occur as long as the downstream factors are recruited prior to dissociation of the DNA glycosylase(s) from the AP-DNA. However, the coupling hypothesis has so far not been investigated in any organism. Such investigations have remained challenging as they require availability of DNA glycosylase mutants whose binding to the AP-sites but not the base excision efficiency or the specificity are affected.

In our earlier studies, we carried out biochemical characterization of Y66W and Y66H mutants of *E. coli* Ung. The activity of the Y66W mutant was not significantly compromised but it was recalcitrant to product inhibition. On the other hand, the Ung activity of the Y66H mutant was severely compromised (~170-fold) but like the wild-type protein it was sensitive to product inhibition (30). We have now, by using equilibrium binding experiments, shown that the Y66W mutant is moderately compromised and attenuated in its binding to AP-DNA (Figure 1D). Thus, the Y66W mutant offered us with a candidate which we could employ to test the physiological significance of the Ung binding to the AP-sites in its overall DNA repair activity. Determination of mutation frequencies suggested that compared to the strain harboring a wild-type *ung* allele, the strains harboring a null, Y66H or Y66W alleles showed increase of about 5.1-, 2.8- and 1.8-folds in the mutation frequencies (Table 2). This observation suggests that despite the fact that the Y66H mutant is compromised in its Ung activity by more than two orders of magnitude it affords a significant rescue of the phenotype of a null strain. Therefore, we reasoned that the Y66W mutant which is merely 7-fold compromised in its Ung activity would have resulted in a better rescue. Hence, it seemed unlikely that the 1.8-fold increase in the mutation frequency of the Y66W strain was merely due to its compromised Ung activity. As the Y66W protein is also attenuated in its AP-DNA binding ability, could its poor AP-DNA binding property somehow contribute to its phenotype? However, as the mutation frequencies do not allow an understanding of the underlying reasons for the observed phenotype, to better understand the mechanism of Y66W mutant, we analyzed the spectrum of mutations leading to acquisition of Rif^R in *E. coli*. A major factor that contributes to Rif^R is the mutations in the RRDR of the *rpoB* gene. Sequence analysis of RRDR from Rif^R colonies arising in different backgrounds (Table 3) showed that while the strain harboring Y66H allele incurred an expected increase in C to T mutations, the strain harboring Y66W allele incurred a remarkable increase in A to G mutations.

In addition, we noted that A to G mutations were predominant even in an AP-endonuclease deficient strain *E. coli* GM7635 which was made ung^+ by introduction of *amp* linked wild-type *ung* allele (*ung*:*amp*, Table 3). Considering that the affinity of the Y66W mutant has been somewhat compromised/attenuated for AP-DNA, this observation suggests that occurrence of A to G mutations could be a consequence of deficient repair of an AP-site. An Ung which is compromised in its binding to AP-site, could leave behind an unshielded AP site against G or an A residue upon excision of uracil from G:U and A:U base pairs, respectively. Although according to the 'A' rule, both the replicative and repair DNA polymerases would predominantly incorporate an 'A' residue against the AP-site, incorporation of 'G' residue could also occur. During replication, incorporation of G against the AP site generated by excision of U from the A:U pair would result in A to G (or T to C) mutations (Supplementary Figure S6A). Likewise, incorporation of A against the AP site generated by excision of U from G:U pair would be seen as G to A (or C to T) mutations (Supplementary Figure S6B). Hence, a deficiency in the residency of the Y66W Ung on the AP-sites, may be expected to result in C to T (despite its efficient Ung activity), and A to G mutations. Although, these two categories of mutations are the major mutations in Y66W background, compared to the wild-type Ung, the frequency of C to T mutations is seen to decrease. It is unclear as to how C to T mutations decrease, but it could merely be a consequence of an increase in A to G mutations which lead to a suppressive effect on the percent values of C to T mutations when considered in a population of Rif^R colonies.

An additional possibility that we considered for an increase in A to G mutations was that the Y66W mutant may have acquired TDG activity and resulted in excision of T from A:T base pairs (41). However, the data shown in Figures 3, 4 and Supplementary Figure S5 clearly rule out such a possibility. Finally, we reasoned that if the TDG or any other unspecific activities were indeed responsible for A to G mutations, expression of wild-type Ung in the *ungY66W*:*amp* background would not result in a decrease of A to G mutation (see 'Results' section). However, as shown in Table 3,

expression of wild-type Ung in the *ungY66W*:*amp* background did result in mitigation of A to G mutations.

Thus, based on our observations with the *E. coli* (*ungY66W*:*amp*) strain, it appears that at least in *E. coli,* binding of Ung to AP-DNA has been optimized for efficient uracil excision repair and functional interaction with the downstream factors. Existence of such a coupling, however, should be viewed as a phenomenon with a critical balance between the processes of rapid recycling of Ung to repair uracil damage in DNA versus the protection of the AP-sites by Ung. A higher affinity binding of Ung to AP-sites may even slow down both the AP-site repair by the AP-endonucleases as well as uracil excision because of slower rates of recycling of Ung. And, the relative affinities of the DNA glycosylases with the substrate, AP-DNA, and their functional interactions with the downstream factors such as the AP-endonucleases must have been a well optimized and carefully evolved phenomenon in the context of the abundance of the remaining DNA repair proteins.

SUPPLEMENTARY DATA

Supplementary Data are available at NAR Online.

ACKNOWLEDGEMENTS

We thank Mr Alok Sharma of the Molecular Biophysics Unit, Indian Institute of Science, Bangalore for helping us with the modeling of thymine into the Ung proteins.

FUNDING

Department of Biotechnology; Department of Science and Technology; the Council of Scientific and Industrial Research (CSIR), New Delhi, India. Funding for open access charge: Government of India.

Conflict of interest statement. None declared.

REFERENCES

1. Friedberg,E.C., Walker,G.C. and Siege,W. (1995) *DNA Repair and Mutagenesis*. ASM Press, Washington, DC.
2. Lindahl,T. (1974) An N-glycosidase from *Escherichia coli* that releases free uracil from DNA containing deaminated cytosine residues. *Proc. Natl Acad. Sci. USA*, **71**, 3649–3653.
3. Lindahl,T., Ljungquist,S., Siegert,W., Nyberg,B. and Sperens,B. (1977) DNA N-glycosidases: properties of uracil-DNA glycosidase from *Escherichia coli*. *J. Biol. Chem.*, **252**, 3286–3294.
4. Aravind,L. and Koonin,E.V. (2000) The alpha/beta fold uracil DNA glycosylases: a common origin with diverse fates. *Genome Biol.*, **1**, 1–8.
5. Krokan,H.E., Standal,R. and Slupphaug,G. (1997) DNA glycosylases in the base excision repair of DNA. *Biochem. J.*, **325**, 1–16.
6. Domena,J.D., Timmer,R.T., Dicharry,S.A. and Mosbaugh,D.W. (1988) Purification and properties of mitochondrial uracil-DNA glycosylase from rat liver. *Biochemistry*, **27**, 6742–6751.
7. Blaisdell,P. and Warner,H. (1983) Partial purification and characterization of a uracil-DNA glycosylase from wheat germ. *J. Biol. Chem.*, **258**, 1603–1609.
8. Williams,M.V. and Pollack,J.D. (1990) A mollicute (mycoplasma) DNA repair enzyme: purification and characterization of uracil-DNA glycosylase. *J. Bacteriol.*, **172**, 2979–2985.
9. Caradonna,S.J. and Cheng,Y.C. (1980) Uracil DNA-glycosylase. Purification and properties of this enzyme isolated from blast cells of acute myelocytic leukemia patients. *J. Biol. Chem.*, **255**, 2293–2300.
10. Talpaert-Borle,M., Campagnari,F. and Creissen,D.M. (1982) Properties of purified uracil-DNA glycosylase from calf thymus. An in vitro study using synthetic DNA-like substrates. *J. Biol. Chem.*, **257**, 1208–1214.
11. Cone,R., Bonura,T. and Friedberg,E.C. (1980) Inhibitor of uracil-DNA glycosylase induced by bacteriophage PBS2. Purification and preliminary characterization. *J. Biol. Chem.*, **255**, 10354–10358.
12. Ravishankar,R., Bidya Sagar,M., Roy,S., Purnapatre,K., Handa,P., Varshney,U. and Vijayan,M. (1998) X-ray analysis of a complex of *Escherichia coli uracil* DNA glycosylase (EcUDG) with a proteinaceous inhibitor. The structure elucidation of a prokaryotic UDG. *Nucleic Acids Res.*, **26**, 4880–4887.
13. Putnam,C.D., Shroyer,M.J., Lundquist,A.J., Mol,C.D., Arvai,A.S., Mosbaugh,D.W. and Tainer,J.A. (1999) Protein mimicry of DNA from crystal structures of the uracil-DNA glycosylase inhibitor protein and its complex with *Escherichia coli* uracil-DNA glycosylase. *J. Mol. Biol.*, **287**, 331–346.
14. Handa,P., Roy,S. and Varshney,U. (2001) The role of leucine 191 of *Escherichia coli* uracil DNA glycosylase in the formation of a highly stable complex with the substrate mimic, ugi, and in uracil excision from the synthetic substrates. *J. Biol. Chem.*, **276**, 17324–17331.
15. Lindahl,T. (1990) Repair of intrinsic DNA lesions. *Mutat. Res.*, **238**, 305–311.
16. Dianov,G., Price,A. and Lindahl,T. (1992) Generation of single-nucleotide repair patches following excision of uracil residue from DNA. *Mol. Cell. Biol.*, **12**, 1605–1612.
17. Dianov,G. and Lindahl,T. (2004) Reconstitution of DNA base excision-repair pathway. *Curr. Biol.*, **12**, 1069–1076.
18. Graves,R.J., Felzenszwalb,I., Laval,J. and O'Connor,T.R. (1992) Excision of 5′-terminal deoxyribose phosphate from damaged DNA is catalyzed by the Fpg protein of *E. coli*. *J. Biol. Chem.*, **267**, 14429–14435.
19. Warner,H.R., Demple,B.F., Deutsch,W.A., Kane,C.M. and Linn,S. (1980) Apurinic/apyrimidinic endonucleases in repair of pyrimidine dimers and other lesions in DNA. *Proc. Natl Acad. Sci. USA*, **77**, 4602–4606.
20. Demple,B., Johnson,A. and Fung,D. (1986) Exonuclease III and endonuclease IV remove 3′ blocks from DNA synthesis primers in H_2O_2-damaged *Escherichia coli*. *Proc. Natl Acad. Sci. USA*, **83**, 7731–7735.
21. Lin,J.J. and Sancar,A. (1989) A new mechanism for repairing oxidative damage to DNA: (A)BC excinuclease removes AP sites and thymine glycols from DNA. *Biochemistry*, **28**, 7979–7984.
22. Snowden,A., Kow,Y.W. and Van Houten,B. (1990) Damage repertoire of the *Escherichia coli* UvrABC nuclease complex includes abasic sites, base-damage analogues, and lesions containing adjacent 5′ or 3′ nicks. *Biochemistry*, **29**, 7251–7259.
23. Lindahl,T. (1982) DNA repair enzymes. *Annu. Rev. Biochem.*, **51**, 61–87.
24. Loeb,L.A. and Preston,B.D. (1986) Mutagenesis by apurinic/apyrimidinic sites. *Annu. Rev. Genet.*, **20**, 201–230.
25. Guillet,M. and Boiteux,S. (2002) Endogenous DNA abasic sites cause cell death in the absence of Apn1, Apn2 and Rad1/Rad10 in *Saccharomyces cerevisiae*. *EMBO J.*, **21**, 2833–2841.
26. Yu,S.L., Lee,S.K., Johnson,R.E., Prakash,L. and Prakash,S. (2003) The stalling of transcription at abasic sites is highly mutagenic. *Mol. Cell. Biol.*, **23**, 382–388.
27. Parikh,S.S., Mol,C.D., Slupphaug,G., Bharati,S., Krokan,H.E. and Tainer,J.A. (1998) Base excision repair initiation revealed by crystal structures and binding kinetics of human uracil-DNA glycosylase with DNA. *EMBO J.*, **17**, 5214–5226.
28. Waters,T.R., Gallinari,P., Jiricny,J. and Swann,P.F. (1999) Human thymine DNA glycosylase binds to apurinic sites in DNA but is displaced by human apurinic endonuclease 1. *J. Biol. Chem.*, **274**, 67–74.

29. Krusong,K., Carpenter,E.P., Bellamy,S.R., Savva,R. and Baldwin,G.S. (2006) A comparative study of uracil-DNA glycosylases from human and herpes simplex virus type 1. *J. Biol. Chem.*, **281**, 4983–4992.
30. Acharya,N., Talawar,R.K., Saikrishnan,K., Vijayan,M. and Varshney,U. (2003) Substitutions at tyrosine 66 of *Escherichia coli* uracil DNA glycosylase lead to characterization of an efficient enzyme that is recalcitrant to product inhibition. *Nucleic Acids Res.*, **31**, 7216–7226.
31. Handa,P., Acharya,N. and Varshney,U. (2002) Effects of mutations at tyrosine 66 and asparagine 123 in the active site pocket of *Escherichia coli* uracil DNA glycosylase on uracil excision from synthetic DNA oligomers: evidence for the occurrence of long-range interactions between the enzyme and substrate. *Nucleic Acids Res.*, **30**, 3086–3095.
32. Kavli,B., Slupphaug,G., Mol,C.D., Arvai,A.S., Peterson,S.B., Tainer,J.A. and Krokan,H.E. (1996) Excision of cytosine and thymine from DNA by mutants of human uracil-DNA glycosylase. *EMBO J.*, **15**, 3442–3447.
33. Datsenko,K.A. and Wanner,B.L. (2000) One-step inactivation of chromosomal genes in *Escherichia coli* K-12 using PCR products. *Proc. Natl Acad. Sci. USA*, **97**, 6640–6645.
34. Miller,J.H. (1972) Generalized transduction use of P1 in strain construction. *Experiments in Molecular Genetics*. Cold Spring Harbor Laboratory, Cold Spring Harbor, NY, pp. 201–205.
35. Spek,E.J., Vuong,L.N., Matsuguchi,T., Marinus,M.G. and Engelward,B.P. (2002) Nitric oxide-induced homologous recombination in *Escherichia coli* is promoted by DNA glycosylases. *J. Bacteriol.*, **184**, 3501–3507.
36. Acharya,N., Kumar,P. and Varshney,U. (2003) Complexes of the uracil-DNA glycosylase inhibitor protein, Ugi, with *Mycobacterium smegmatis* and *Mycobacterium tuberculosis* uracil-DNA glycosylases. *Microbiology*, **149**, 1647–1658.
37. Sohail,A., Klapacz,J., Samaranayake,M., Ullah,A. and Bhagwat,A.S. (2003) Human activation-induced cytidine deaminase causes transcription-dependent, strand-biased C to U deaminations. *Nucleic Acids Res.*, **31**, 2990–2994.
38. Emsley,P. and Cowtan,K. (2004) Coot: model-building tools for molecular graphics. *Acta Crystallogr. D Biol. Crystallogr.*, **60**, 2126–2132.
39. Van Der Spoel,D., Lindahl,E., Hess,B., Groenhof,G., Mark,A.E. and Berendsen,H.J. (2005) GROMACS: fast, flexible, and free. *J. Comput. Chem.*, **26**, 1701–1718.
40. Handa,P., Acharya,N., Thanedar,S., Purnapatre,K. and Varshney,U. (2000) Distinct properties of *Mycobacterium tuberculosis* single-stranded DNA binding protein and its functional characterization in *Escherichia coli*. *Nucleic Acids Res.*, **28**, 3823–3829.
41. Otterlei,M., Kavli,B., Standal,R., Skjelbred,C., Bharati,S. and Krokan,H.E. (2000) Repair of chromosomal abasic sites *in vivo* involves at least three different repair pathways. *EMBO J.*, **19**, 5542–5551.
42. Payne,R.C. and Traut,T.W. (1982) The complete separation of the base, nucleoside, mono-, di-, and triphosphonucleosides of uracil and cytosine by polyethyleneimine cellulose thin-layer chromatography. *Anal. Biochem.*, **121**, 49–54.
43. Sambrook,J., Fritsch,E.F. and Maniatis,T. (1989) *Molecular Cloning: A Laboratory Manual*, 2nd edn. Cold Spring Harbor Laboratory, Cold Spring Harbor, NY.
44. Reid,S.L., Parry,D., Liu,H.H. and Connolly,B.A. (2001) Binding and recognition of GATATC target sequences by the EcoRV restriction endonuclease: a study using fluorescent oligonucleotides and fluorescence polarization. *Biochemistry*, **40**, 2484–2494.
45. Venkatesh,J., Kumar,P., Krishna,P.S., Manjunath,R. and Varshney,U. (2003) Importance of uracil DNA glycosylase in *Pseudomonas aeruginosa* and *Mycobacterium smegmatis*, G+C-rich bacteria, in mutation prevention, tolerance to acidified nitrite, and endurance in mouse macrophages. *J. Biol. Chem.*, **278**, 24350–24358.
46. Srinath,T., Bharti,S.K. and Varshney,U. (2007) Substrate specificities and functional characterization of a thermo-tolerant uracil DNA glycosylase (UdgB) from *Mycobacterium tuberculosis*. *DNA Repair*, **6**, 1517–1528.
47. Fels,A.O. and Cohn,Z.A. (1986) The alveolar macrophage. *J. Appl. Physiol.*, **60**, 353–369.
48. Lancaster,J.R. Jr (1996) Diffusion of free nitric oxide. *Methods Enzymol.*, **268**, 31–50.
49. Imlay,J.A. (2003) Pathways of oxidative damage. *Annu. Rev. Microbiol.*, **57**, 395–418.
50. Pope,M.A., Porello,S.L. and David,S.S. (2002) *Escherichia coli* apurinic-apyrimidinic endonucleases enhance the turnover of the adenine glycosylase MutY with G:A substrates. *J. Biol. Chem.*, **277**, 22605–22615.
51. Lu,A.L., Lee,C.Y., Li,L. and Li,X. (2006) Physical and functional interactions between *Escherichia coli* MutY and endonuclease VIII. *Biochem. J.*, **393**, 381–387.
52. Barrett,T.E., Scharer,O.D., Savva,R., Brown,T., Jiricny,J., Verdine,G.L. and Pearl,L.H. (1999) Crystal structure of a thwarted mismatch glycosylase DNA repair complex. *EMBO J.*, **18**, 6599–6609.
53. Yu,D., Ellis,H.M., Lee,E.C., Jenkins,N.A., Copeland,N.G. and Court,D.L. (2000) An efficient recombination system for chromosome engineering in *Escherichia coli*. *Proc. Natl Acad. Sci. USA*, **97**, 5978–5983.
54. Blattner,F.R., Plunkett,G. III, Bloch,C.A., Perna,N.T., Burland,V., Riley,M., Collado-Vides,J., Glasner,J.D., Rode,C.K., Mayhew,G.F. *et al.* (1997) The complete genome sequence of *Escherichia coli* K-12. *Science*, **277**, 1453–1462.
55. Vieira,J. and Messing,J. (1982) The pUC plasmids, an M13mp7-derived system for insertion mutagenesis and sequencing with synthetic universal primers. *Gene*, **19**, 259–268.
56. Roy,S., Purnapatre,K., Handa,P., Boyanapalli,M. and Varshney,U. (1998) Use of a coupled transcriptional system for consistent overexpression and purification of UDG-Ugi complex and Ugi from *Escherichia coli*. *Protein Expr. Purif.*, **13**, 155–162.